Artificial Organs

A Soft Total Artificial Heart—First Concept Evaluation on a Hybrid Mock Circulation

*Nicholas H. Cohrs, †Anastasios Petrou, *Michael Loepfe, *Maria Yliruka, *Christoph M. Schumacher, *A. Xavier Kohll, ‡Christoph T. Starck, †Marianne Schmid Daners, †Mirko Meboldt, ‡Volkmar Falk, and *Wendelin J. Stark

*Institute for Chemical and Bioengineering, ETH Zurich; †Product Development Group Zurich, Department of Mechanical and Process Engineering, ETH Zurich, Zurich, Switzerland; and ‡Department for Cardiothoracic and Vascular Surgery, Deutsches Herzzentrum Berlin, Berlin, Germany

Abstract: The technology of 3D-printing has allowed the production of entirely soft pumps with complex chamber geometries. We used this technique to develop a completely soft pneumatically driven total artificial heart from silicone elastomers and evaluated its performance on a hybrid mock circulation. The goal of this study is to present an innovative concept of a soft total artificial heart (sTAH). Using the form of a human heart, we designed a sTAH, which consists of only two ventricles and produced it using a 3D-printing, lost-wax casting technique. The diastolic properties of the sTAH were defined and the performance of the sTAH was evaluated on a hybrid mock circulation under various physiological conditions. The sTAH achieved a blood flow of 2.2 L/min against a systemic vascular resistance of 1.11 mm Hg s/mL (afterload), when operated at 80 bpm. At the same time, the mean pulmonary venous pressure (preload) was fixed at 10 mm Hg. Furthermore, an aortic pulse pressure of 35 mm Hg was measured, with a mean aortic pressure of 48 mm Hg. The sTAH generated physiologically shaped signals of blood flow and pressures by mimicking the movement of a real heart. The preliminary results of this study show a promising potential of the soft pumps in heart replacements. Further work, focused on increasing blood flow and in turn aortic pressure is required. **Key Words:** Soft pump—Total artificial heart—Hybrid mock simulation—Physiological—3D-printing.

The number of deaths from cardiovascular diseases keeps on growing, reaching a share of approximately 30% of all deaths worldwide. Heart failure (HF) affects more than 26 million people worldwide (1). Even in developing countries, the number of HF patients is continuously increasing (1). The necessity to treat HF and the shortage of donor hearts led to the development of mechanical circulatory support devices, such as ventricular assist devices (VADs) and total artificial hearts (TAHs).

VADs are implantable mechanical pumps that support the heart of HF patients. They can be placed in the left, right, or both ventricles but mostly in the left ventricle (LV). Left VAD (LVAD) treatment has dramatically evolved over the last decade, reaching a number of 5000 devices/year, with 1- and 2-year survival rates equal to 80 and 70%, respectively (2). However, adverse events, such as hemolysis and thrombosis, as well as infections, still occur and prevent VADs from being established as the gold standard for HF treatment. Prolonged hospital stays resulting from adverse events dramatically increase the cost of therapy. Therefore, the elimination of these complications needs to be addressed in the future. Furthermore the quality of life of VAD patients may be significantly improved by minimizing the number of adverse events.

doi: 10.1111/aor.12956

Received September 2016; revised March 2017; accepted March 2017.

The first two authors contributed equally to this work.

Address correspondence and reprint requests to Prof. Dr. Wendelin J. Stark, ETH Zurich, Institute for Chemical and Bioengineering, Vladimir-Prelog-Weg 1, 8093 Zurich, Switzerland. E-mail: wstark@ethz.ch

One major adverse event is right ventricular (RV) failure following LVAD implantation. A range of 10–50% of all LVAD patients suffers from postoperative RV failure and when medical therapy does not suffice to support adequately the RV, temporary or permanent mechanical support is required (3). In patients with biventricular heart failure primary biventricular VAD (BiVAD) support may be necessary. However, the survival rates of BiVAD support remain significantly lower than the survival rates of patients receiving merely LVAD support (4,5).

An alternative treatment option for long-term support of both ventricles is the TAH. A TAH is a single device with two integrated pumps. Today, the SynCardia TAH (SynCardia Systems, Inc., Tucson, AZ, USA) is the only pulsatile TAH which is approved by the Food and Drug Administration (FDA) in the United States as a bridge to transplantation therapy and has acquired the CE mark in Europe. Thus far, more than 1,400 TAH implantations have been conducted. The 1-year survival rate of TAH patients is approximately 60–79%, but on average still much lower compared with LVAD patients (2,6). However, several TAHs are currently under development, aiming at further improving the TAH treatment. The CARMAT TAH (CARMAT, Velizy Villacoublay, France) is under clinical investigations, while the ReinHeart TAH (ReinHeart TAH GmbH, Gütersloh, Germany), the continuous flow Cleveland Clinic CFTAH (Cleveland, OH, USA), and the BiVACOR (BiVACOR, Inc., Houston, TX, USA) are under evaluation through chronic animal trials (7–10).

All existing VADs and TAHs consist of many mechanical parts, being thrombogenic when in contact with blood. Therefore, to prevent thromboembolic complications, both VAD and TAH treatment require anticoagulation therapy. The risk of thromboembolism and the need for anticoagulation therapy with the inherent risk of bleeding complications are one of the major backdraws of current VAD and TAH systems (11).

Recently, the field of soft technologies has driven considerable attention (12–14). In this field different completely soft pumps have been presented, which are manufactured by a 3D-printing, lost-wax casting technique (15,16). This process allows the low cost production of pumps of silicone monoblocks with complex chamber design, without any seams and mechanical parts. In 2014, Schumacher et al. presented a combustion-driven soft pump, which showed human heart-like pumping characteristics (15). In this study, we present a novel concept of a pneumatically driven TAH, which is made of one silicone elastomer monoblock and thus, is completely soft. This technology aims at replicating biomimetic motion of soft muscular systems using bending, twisting extension, and flexion (14,17). Thus, the soft TAH (sTAH) should mimic the human heart from a physiological and physical motion point of view, yielding pulsatile blood flow (17). The study is structured as follows. First, we explain in detail the design and production process of the sTAH. Then, the evaluation process of the sTAH on a hybrid mock circulation (HMC) is described. Third, the resulting performance of the TAH during pre- and afterload experiments is presented. Finally, the overall performance of the TAH is analyzed and its potential as a future HF treatment option is discussed.

MATERIALS AND METHODS

Design of the soft total artificial heart

Figure 1 shows the general design procedure of the sTAH. We used a computer aided design (CAD) file of a real human heart to copy its physiological form (Fig. 1a). As a first step, we used a CAD software

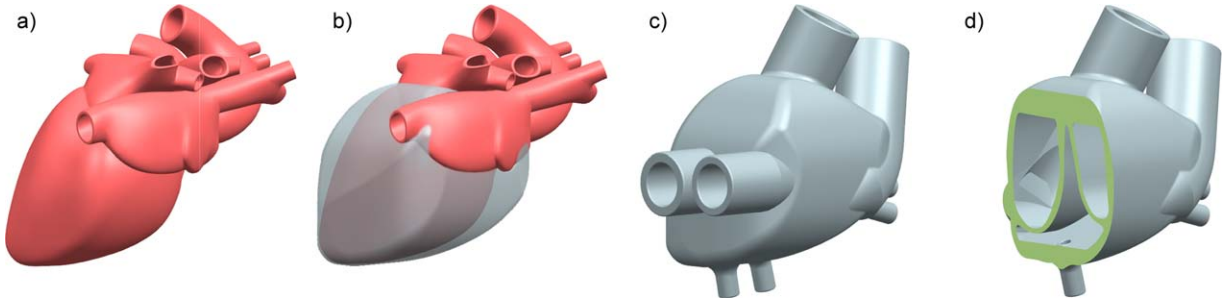

FIG. 1. Illustration of the design procedure for the soft total artificial heart (sTAH). The computer model of a human heart (a) is used to give the outer shape of the sTAH. (b) This shape is used as a basis and extended by adding chambers (d) and in- and outflows to and from the chambers, which gives the final form of the sTAH (c).

(NX8.5, Siemens, Munich, Germany) and the respective CAD-file of a healthy human heart. This helped to design the outer form of the sTAH with a similar shape as a real human heart, excluding the aorta, the pulmonary artery, and the pulmonary and caval veins (Fig. 1b). To reduce the complexity of the system, we designed the chambers without atriums, thereby creating two ventricles with sizes of 144 cm^3 and 83 cm^3 for the LV and RV, respectively. In comparison with the human heart, we placed the inflow to the heart chambers at the posterior aspect as the artificial heart does not comprise atriums. The diameter of the inflow to the ventricles was chosen as 24 mm. We placed the outflow (diameter 30 mm) from the ventricles in anatomic correct positions to facilitate connection to the aorta and the pulmonary artery (Fig. 1c). The pneumatically driven expansion chamber (EC) was placed between the ventricles to allow simultaneous pumping from both chambers (Fig. 1d). This addition of another chamber reduced the volumetric size of the right ventricle. Four ports to the EC with diameters of 6 mm were added. These are used for the in- and deflation of the EC (Fig. 2). Two ports to the EC were placed at the apex, while the two remaining ones were placed at the back of the heart. The EC contained four ports, because the sTAH was initially designed to be run by combustion, which required four ports. Table 1 gives the volumetric sizes of the sTAH. Additional detailed sketches of the sTAH, including wall thicknesses and dimensions are available in the supporting information.

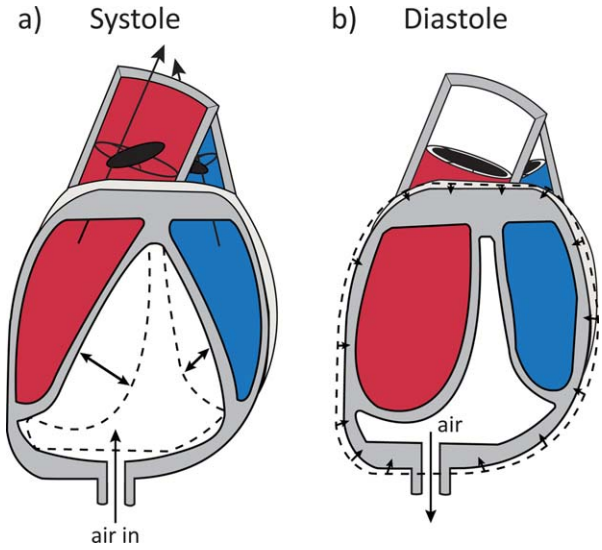

FIG. 2. Representation of the drive of the presented soft total artificial heart (sTAH). (a) Depiction of systole: pressurized air inflates the expansion chamber (EC), thereby displacing the blood and yielding a pulsatile flow towards the arteries. (b) Depiction of diastole: the pressure in the EC is relieved, which causes a pressure drop in the ventricles and finally results in a heart valve–directed refilling of the chambers with blood.

TABLE 1. *Summary of the volumetric sizes of the soft total artificial heart (sTAH), its main body without the in- and outlets and its chambers*

Description	Volumetric size/cm^3
sTAH	679
LV	144
RV	83
EC	70
sTAH minus chambers (silicone only)	382
Main body	592
Main body minus chambers (silicone only)	294

LV, left ventricle; RV, right ventricle; EC, expansion chamber.

Production of the soft total artificial heart

The sTAH was prepared by a lost-wax casting method, which had already been presented from our group (15). A detailed description of the manufacturing process is available in the supporting information. Briefly, an injection mold of the designed heart was produced of poly(acrylonitrile-*co*-butadiene-*co*-styrene)-plastic (ABS) using 3D-printing. The voids were filled with room temperature vulcanizing (RTV) silicone and cured at room temperature for 12 h and afterwards at 65°C in an oven for at least 24 h. Thereafter, the ABS mold was dissolved in an acetone bath, which gave the sTAH made of one single silicone monoblock. To direct the flow, mechanical heart valves (Björk-Shiley type) with a diameter of 23 mm, surrounded by rubber rings were clamped into the in- and outlets of the ventricles using laces. The tensile properties of the used silicone elastomer were determined according to the DIN 53504 norm.

Actuation of the soft total artificial heart

The sTAH is driven pneumatically by inflating and deflating the EC between the two ventricles using pressurized air at 2 bar. Figure 2 illustrates this operation-principle. During systole, the EC is pressurized (Fig. 2a). Thus, the EC expands and thereby presses the blood from both left and right heart chambers towards the aorta and pulmonary artery, respectively. During diastole (Fig. 2b), the EC relaxes as the pressure is relieved and the heart moves back to its initial shape. The outflow valves close, while the inflow valves open and the ventricles are refilled by the preload. In contrast to existing pulsatile TAHs, the presented sTAH expands and shrinks during pumping due to its entire softness. The technical details, including types of valves and controller and

in- and deflation times of the pneumatic drive are provided in the supporting information.

Hybrid mock circulation

The sTAH was evaluated on a HMC (18), which uses a validated numerical model of the human blood circulation (19). This HMC has been developed for evaluating LVADs and therefore, had to be modified to conduct our experiments with the sTAH. However, the modified HMC is able to test one side of the sTAH at every experiment. Figure 3a illustrates the possible placement of the sTAH on a human blood circulation. The RV of the sTAH pumps from the systemic venous system to the pulmonary arterial system, while the LV pumps from the pulmonary venous system to the systemic arterial system. Figure 3b shows how the human blood circulation is mimicked on the modified HMC to evaluate the sTAH.

The modified HMC can be divided into two parts: the passive and the active part. The passive part was used to simulate constant physiological conditions for the right side of the sTAH. It consists of a bucket and tubes, which are placed such that a hydrostatic pressure difference of 40 mm Hg is applied for the RV of the sTAH. The active part consists of the HMC, which was used to simulate varying physiological conditions on the LV of the sTAH (18). Specifically, two pressure-controlled reservoirs were used to simulate the pulmonary venous pressure (PVP) and the aortic pressure (AoP). The reference signals for the air pressure controllers (PVP_{ref} and AoP_{ref}) of the two reservoirs were computed in real time by a numerical model of the pulmonary and systemic circulations

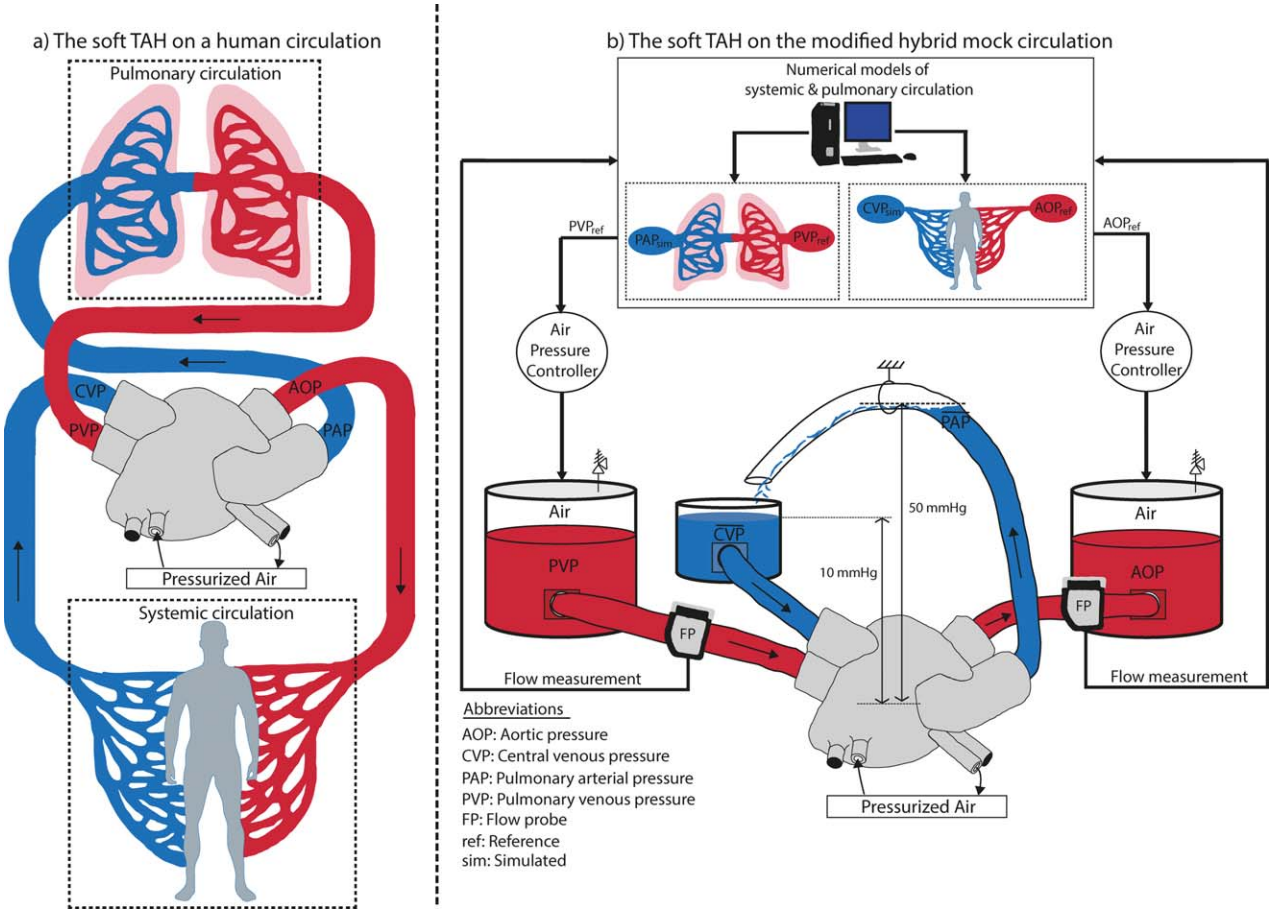

FIG. 3. (a) Illustration of the soft total artificial heart (sTAH) on a human circulation. The right ventricle (RV) pumps from the systemic venous system to the pulmonary arterial system, while the left ventricle (LV) pumps from the pulmonary venous system to the systemic arterial system. (b) Illustration of the hybrid mock circulation (HMC) (14) which was used to evaluate the sTAH. In the current setup, the LV of the sTAH is connected to the HMC. The HMC uses a real-time numerical model of the systemic and pulmonary circulations to apply the pulmonary venous pressure (PVP) and the aortic pressure (AOP) in the pressure-controlled reservoirs. The RV of the sTAH is connected to a passive hydraulic system that simulates a hydrostatic pressure difference of 40 mm Hg.

based on the inlet and outlet flows of the LV of the sTAH. These flows are measured by ultrasonic flow probes and recorded at 1 kHz (Fig. 3). Due to the lack of the interaction of the RV of the sTAH with the numerical model, we had to define the RV inlet and outlet pressures. Therefore, we set and kept constant the central venous pressure (CVP) of the numerical model (CVP_{sim}) equal to 7 mm Hg, whereas the simulated pulmonary arterial pressure (PAP_{sim}) was adjusted by a defined pulmonary vascular resistance of 0.1 mm Hg s/mL. The schematic of the numerical model is provided in detail in the supporting information, as well as a movie that shows the actuated sTAH during the experiments on the modified HMC.

For this study, we only present results for the left sTAH. The reasons for not presenting the performance of the right sTAH are explained in the discussion section. We used three sTAH to conduct the experiments.

Experiments

We used the modified HMC to conduct two sets of experiments. The first set included the characterization of the sTAH. For this purpose, the performance of the sTAH with the current actuation system was evaluated while keeping a constant inlet pressure and increasing stepwise the outlet pressure. This experiment was repeated at different heart rates, which varied from 60 bpm to 120 bpm with a stepsize of 10 bpm. The pressure difference–flow (H-Q) relationship for different pumping rates was derived, where the pressure difference is the difference between the mean inlet and outlet pressures. In addition, the diastolic properties of the right and left sTAH were defined. For this purpose, we stepwise increased the volume of each chamber separately by 5 mL and measured the generated pressure at each step. The sTAH was at a nonejecting mode of operation.

The second set of experiments included pre- and afterload variation experiments. To vary the preload, we increased the PVP from 3 mm Hg to 30 mm Hg with an increment of 3 mm Hg every 10 s, such that we always achieved steady state conditions. At the same time, the afterload was fixed by keeping the systemic vascular resistance (SVR) equal to 1.11 mm Hg s/mL. For the afterload variation experiment we increased the SVR from 0.2 mm Hg s/mL to 2.1 mm Hg s/mL with an increment of 0.1 mm Hg s/mL again every 10 s. Similarly, the preload was fixed by setting the PVP equal to 10 mm Hg. The supporting information included a detailed table (Table S4), which gives the specific values for SVR, PVP, pulmonary vascular resistance, and central venous pressure for each experiment conducted. For all experiments a glycerol water mixture with a viscosity of 2.8 MPa s was used to mimic the blood viscosity.

Durability problems of the material of the sTAH prevented us from completing all experiments. Therefore, we present results only regarding the H-Q curves, the afterload variation experiment at 60, 70, and 80 bpm, and the preload variation experiment at 60 and 70 bpm.

RESULTS

The production process yielded an entirely soft artificial heart (except the mechanical heart valves) with a mass of 390 g and a size of 1.25 times the original heart size by volume, even though no atriums were included (see Fig. 1a). The volumetric sizes of the sTAH are summarized in Table 1. The elastic modulus E of the silicone was measured as $E = 2.98 \pm 0.16$ MPa ($n = 5$). Additional geometrical data, including sketches as well as mechanical properties are available in the supporting information.

Pump performance

Figure 4 shows the generated flow from the LV against an increasing pressure difference for different heart rates with the used actuation system. The flow generally increases for higher heart rates and

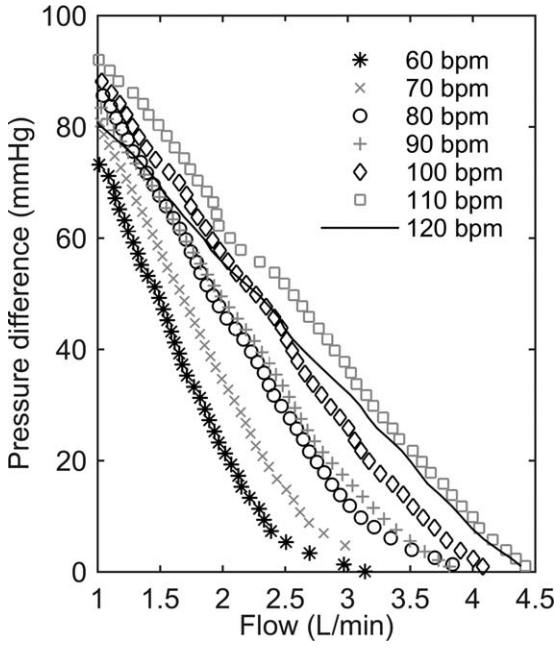

FIG. 4. Pressure difference over flow diagram of the left ventricle of the soft total artificial heart (sTAH) for different heart rates.

TABLE 2. *Calculated root-mean-square-error (RMSE) in left heart flow in L/min between all three sTAH prototypes used for H-Q experiments*

Operated heartbeat	$sTAH_1$ versus $sTAH_2$ (L/min)	$sTAH_1$ versus $sTAH_3$ (L/min)	$sTAH_2$ versus $sTAH_3$ (L/min)
60 bpm	0.15	0.15	0.07
70 bpm	0.19	0.11	0.11
80 bpm	0.25	0.24	0.10
90 bpm	0.32	0.20	0.15
100 bpm	0.24	0.25	0.11

smaller pressure differences. At 110 bpm, a maximum flow of 4.5 L/min can be reached at zero pressure. At realistic physiological pressure difference conditions (90 mm Hg), the blood flow is limited to approximately 1 L/min. For heart rates larger than 110 bpm, the characteristics of the heart change. In these cases, the blood flow increases with a smaller slope with decreasing pressure difference, compared with heart rates below 110 bpm. This results in lower flows at physiological pressure difference conditions for large heart rates. Similar performance was derived with each of the three tested prototypes. Table 2 lists the root-mean-square-error (RMSE) of left heart flow within the same pressure difference between each prototype. The difference is considered negligible. The H-Q curves for each prototype are included in the supporting information.

Figure 5 depicts the relationship between pressure and volume for both sides of the non-ejecting sTAH. For the right sTAH, a pressure of 20 mm Hg was achieved at 98 mL, whereas for the left sTAH this pressure was achieved at 147 mL. Both curves present a steep increase in pressure while the filling volume increases.

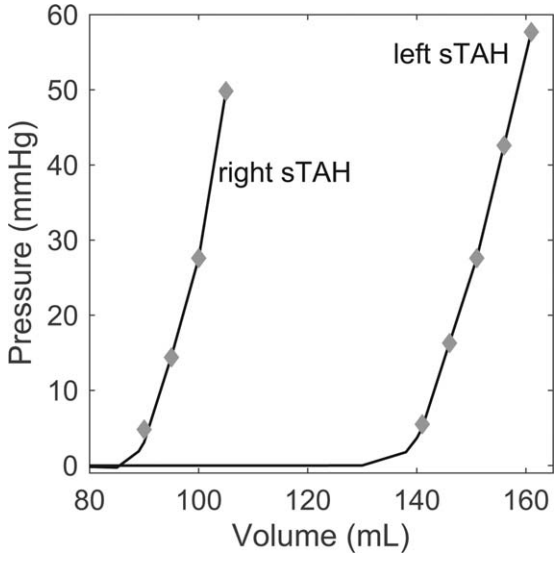

FIG. 5. Diastolic pressure versus volume relationship of the non-ejecting right and left sides of the soft total artificial heart (sTAH).

Use as an artificial heart

Figure 6 shows the measured flow- and pressure signal during an afterload experiment of the LV at an operated heart rate of 80 bpm. At physiological afterload, that is SVR equal to 1.11 mm Hg s/mL, the presented sTAH reached a systolic aortic pressure of 71 mm Hg, while the diastolic pressure was equal to 36 mm Hg. Thus, an aortic pulse pressure (AoPP) of 35 mm Hg was recorded. The corresponding peak aortic flow from the LV was 15 L/min, with an LV flow of 2.2 L/min, which yielded to a stroke volume of 27.5 mL. The backflow

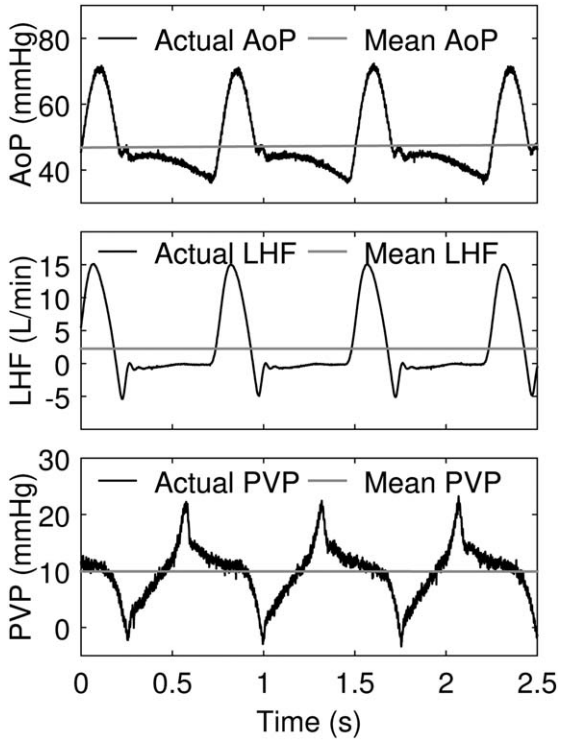

FIG. 6. Beat-by-beat performance of the soft total artificial heart (sTAH), with a heart rate of 80 bpm, when pumping against and systemic vascular resistance of 1.11 mm Hg s/mL. It shows the measured signals of the aortic pressure (AoP), the left ventricular flow (LVF), and the pulmonary venous pressure (PVP).

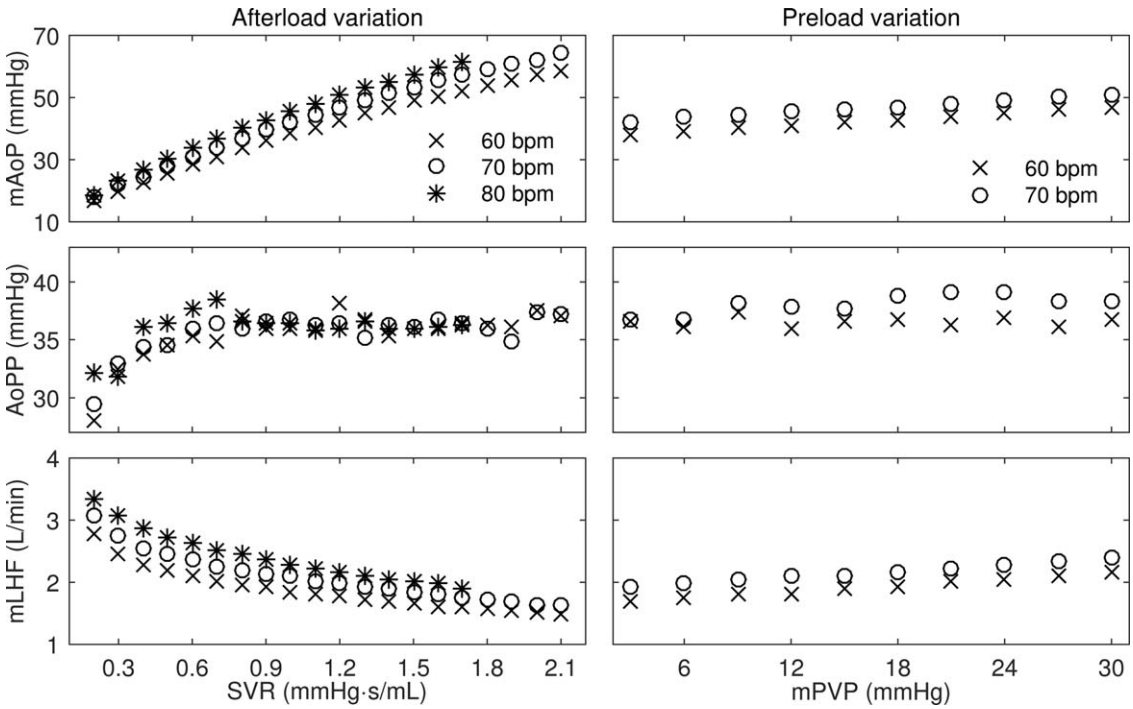

FIG. 7. Performance results of the left ventricle of the soft total artificial heart (sTAH) during after- and preload variation experiments for different heart rates. The signal of the mean aortic pressure (mAoP), the aortic pulse pressure (AoPP), and the mean left ventricular flow (mLVF) are depicted as a function of physiological systemic vascular resistances (SVR) during afterload variations and as a function of mean pulmonary venous pressure (mPVP) during preload variations. The experiments were interrupted during afterload variation and at 80 bpm at 1.7 mm Hg s/mL due to rupture of the sTAH.

reached up to −5 L/min during diastole until the mechanical heart valves closed. The flow remained negative during diastole, due to the characteristics of the mechanical heart valves, which allow backflow to prevent thrombus formation.

Figure 7 presents the mean aortic pressure (mAoP), AoPP, and the mean LV flow (mLVF) during all conducted pre- and afterload experiments. In both variations, the mAoP as well as the mLVF increased with increasing heart rate. For afterload variations, at every fixed heart rate, the mAoP increased, while the SVR was increasing, whereas the LV flow gradually decreased. The AoPP increased with increasing SVR, but plateaued at approximately 36 mm Hg for SVRs larger than 0.6 mm Hg s/mL. In addition, it seems to be independent of the heart rate, as it plateaued at the similar value for all measured heart rates. In the case of preload variations, the mAoP and mLVF increased gradually with increasing mean pulmonary venous pressure (mPVP). Again, the mAoP and the mLVF were larger for larger heart rates, while there was no clear dependence for the AoPP. Generally, the influence of the preload variation seems smaller than the afterload variations. Furthermore, the lifetime of the sTAH was limited to approximately 3000 beats, as the membrane between the EC and LV ruptured while the sTAH was operated at 80 bpm during the afterload experiment (at SVR equal to 1.7 mm Hg s/mL). Therefore, no further measurements were acquired. This rupture was linear with a size of approximately 2 cm and located at the transition of the internal membrane to the main outer body.

DISCUSSION AND CONCLUSIONS

The goal of this study was not to present a new, readily implantable TAH, but rather a new concept for future artificial heart development. We are at the initial stage of research, but think it is valuable for the medical and engineering communities to present the first results. The measurements show that further progress is needed, but there are also some pioneering results. There are two major advantages of the presented concept: first, the low complexity of the heart and its simple production and second, the influence of the heart's soft material which results in a device replicating the biomimetic motion of the human heart. However, the influence of this soft movement on the blood still has to be evaluated and was not part of this study.

The use of widely available and easy to use design software as well as the production using commercially available 3D-printers could allow a personalized and decentralized production in the heart centers and institutes. As the design can be changed very easily, the sTAH could be adapted to specific physiological properties of the individual patient. In comparison, the newly developed CARMAT TAH is expected to only fit into 65% of all patients (7). In addition, the sTAH is only comprised of silicone elastomers, which are greatly available in medical grades and can be processed easily without the need for expensive and complex equipment. This could be the first step towards a low cost personalized medicine for implants in artificial blood pump therapy. Still, due to political and regulatory issues, this step into the clinical application is currently unlikely in the foreseeable future. However, 3D-printing technology could enable this possible next step in personalized medicine.

The presented sTAH has a size of 679 cm^3, which is too large for implantation due to its outer shape, though we aim for a significant decrease in volume and weight of the implantable part of the sTAH in the future. The goal must be to have the same size as the patient's diseased heart to prevent complications during surgery due to fitting problems. Another shortcoming of our design of the sTAH is a reduced RV volume of 83 cm^3, which was required for the placement of the EC. In this design, this will most likely result in reduced blood flow from the RV to the pulmonary arterial system and thus, yield in reduced blood flow from the pulmonary venous system to the LV. In addition, the presence of only one EC reduces the possibility to control the LV and RV separately and precisely, if different loads are clinically required. These issues will have to be resolved in a next generation sTAH.

Besides the low complexity of the heart and the placement of the parts which are most likely to fail outside the body (valves, air-pump, controller), an advantage is associated to the elastomeric properties of the silicone. The pressurized air causes a movement of the entire heart with every beat because there are no hard, mechanical parts except the valves. In contrast, every existing LVAD and TAH is comprised of at least one rigid, blood contacting surface which does not move (7,20,21).

The entirely soft design of the sTAH allowed us to mimic the physiological movement of the human heart during pumping and thus, to reproduce a physiological blood flow situation. Due to the movement of the entire sTAH structure with every beat, enabled by the softness of the materials, we expect no dead spots of the flow within the sTAH. Dead spots with reduced flow within blood pumps are a major problem as the blood automatically produces thrombin once it is in contact with an artificial surface (22). However, sufficient blood flow dilutes the thrombin concentration, such that no blood clotting can occur. Thus, due to presumable lack of dead spots, caused by the biomimetic motion of the sTAH, we hope to be able to reduce the amount of required anticoagulation, which is the main reason for bleeding complications and one major cause of death (6,22–24). Still, the elastic modulus of the silicone elastomer is greater compared with left ventricular muscle (diastolic: 0.007–0.11 MPa, systolic: 0.027–0.4 MPa [25]). However, the elastic modulus of the material is much less than that of the currently used rigid systems such as IsoPlast engineering thermoplastic polyurethane (26) (elastic modulus IsoPlast: 1500–17 000 MPa [27,28]) and, thus, offers a more physiological situation to the human body. Besides the soft movement of the ventricles, the movement of the entire heart during the beats also seems more natural, compared with the hard TAHs and LVADs (video in the supporting materials). One major disadvantage of the presented heart is the need for a percutaneous driveline, which will lead to known disadvantages of the currently used LVADs and TAHs, such as the danger for infections and reduced quality of life for the patients.

In addition to the pure introduction of a new concept for total artificial hearts, a second goal of this study was to evaluate the performance of the sTAH under physiological conditions. For this purpose, we derived the H-Q characteristics for the LV of the sTAH. In addition, we evaluated the sTAH under various pre- and afterload conditions, when operated at different pumping rates. The pre- and afterload variation experiments provided a broad overview of the pumping performance of the sTAH under possible clinical conditions (Fig. 7). A simulated representative clinical scenario can be found at the left-hand side of Fig. 7, where the mean PVP (preload) was fixed at 10 mm Hg, the SVR was 1.11 mm Hg s/mL and the sTAH pumping rate was 80 bpm. At these conditions the sTAH was able to pump 2.2 L/min, which led to a mAoP of 48 mm Hg and an AoPP of 36 mm Hg. We admit that the generated LV flow and in turn the mAoP are smaller than required for implantation and compared with what other TAHs can achieve. The AoPP can be considered physiological and comparable with other TAHs, which are more

advanced (3,10). However, this has to be reevaluated with a prototype that achieves a physiological mAoP as well, to prove that a possible elevated pulse pressure is avoided. Furthermore, due to the linear relationship between pressure and flow (29), the physiological shape of the signals promises a physiological blood pressure and blood flow, once higher flows can be achieved with a next generation sTAH.

The diastolic properties of the sTAH were defined. Results showed that the sTAH is much stiffer compared with the native heart, that is, the slope is steeper (30), as the pressure greatly increases after a small change in volume. This is also justified by the elastic modulus of the sTAH.

The performance of the left sTAH against an increasing afterload was presented through H-Q curves, when driven by the used actuation system. At pumping rates larger than 110 bpm, the pumping ability of the sTAH was diminished. We believe that for high heart rates, the need for very rapid in- and deflation of the EC influences the movement of the sTAH negatively and causes this reduction in flow and behavior. However, this performance and the resulted linearity of the H-Q curves can be adjusted by modifying the actuation system and using similar technologies to what is currently in clinical use, for example by the Berlin Heart Excor (Berlin Heart GmbH, Berlin, Germany). Thus, the filling and ejection pressures would be defined dynamically to achieve physiological flow conditions.

The experiments were conducted on a modified HMC, which can accurately generate physiological signals (18). The contour of the recorded signals of the LV flow, the AoP, and the PVP resembles the corresponding signals of a human heart (31). Thus, we assume a physiological blood flow waveform due to the biomimicking motion of the sTAH, despite the lower mean flow and pressure values achieved, as compared with the physiological ones. These physiological signals also prove the physiological performance of our modified HMC. Compared with other MC systems used for evaluating TAHs (3,32), our modified MC presents a comparable physiological performance. Furthermore, our modified HMC offers the advantage of implementing easily various physiological conditions, by varying numerical parameters. Therefore, the evaluation of the LV of the sTAH, under various pre- and afterload conditions was feasible by varying the PVP and SVR, respectively. For the RV of the sTAH, a constant strain with a hydrostatic pressure of 40 mm Hg was applied. In HF patients, a systolic PAP of 45–55 mm Hg and diastolic PAP of 20–25 mm Hg can be observed. The applied elevated constant RV strain was used as a substitute for the neglected dynamic effects.

A limitation of our HMC is that it is designed for testing only one hydraulic device at a time and therefore, we were able to evaluate only one ventricle of the sTAH per experiment. We acknowledge the existence of other MC systems which are able to evaluate both sides of a TAH simultaneously (3,32,33). In our study, we tried to estimate the effect of the RV of the sTAH in both the numerical model and the physical prototype, as described in the "Hybrid mock circulation" section. Of course, the pre- and afterload conditions of the RV would change during pre- and afterload variations of the LV. However, this interdependence is not considered to have significant influence to our generated results for the LV of the sTAH.

In this study, no results regarding the performance of the RV of the sTAH are presented. In fact, we were able to switch the connection to the pressure reservoir side of the sTAH, increase the hydrostatic pressure, and properly adjust the numerical model. Thus, the RV of the sTAH would be evaluated, while the LV would pump against a hydrostatic pressure. However, this was not feasible due to limited durability of the sTAH (approximately 3000 beats). The sTAH prototypes ruptured at the membrane which separated the LV from the EC. This seems to be the weak spot of the presented design. Of course, the achieved lifetime differs significantly from the needed 30 to 50 million beats as a first milestone. Still, there is room for vast improvements. Another iteration of the design could remove this weak spot of the membrane separating the LV and the EC, while the use of other, more tear-resistant high performance medical grade polymers could give an additional significant reduction of the problem. Alternative polymers are widely available and can be processed similarly (34). These include elastomeric polyurethanes, which are available in medical grades from multiple suppliers, as well as combinations of polyurethanes with PDMS (34). Also, olefin-based elastomers are available in biomedical grades and, for example, are already used in artificial heart pump diaphragms (34,35). Future developments will address the lack of mechanical stability of the used silicone material. Still, this issue is a game breaker and needs to be resolved.

Acknowledgments: The authors would like to thank Roland Walker for his support. The authors

gratefully acknowledge the financial support by ETH Zurich, the Baugarten Stiftung, the Stavros Niarchos Foundation, and the ETH Zurich Foundation. This work is part of the Zurich Heart Project under the umbrella of "University Medicine Zurich/Hochschulmedizin Zürich."

Conflict of Interest: M.L., C.M.S., and W.J.S. declare the filing of a patent regarding soft pumps. All other authors declare no conflict of interest.

REFERENCES

1. Sunagawa G, Horvath DJ, Karimov JH, Moazami N, Fukamachi K. Future prospects for the total artificial heart. *Expert Rev Med Devices* 2016;13:191–201.
2. Kirklin JK, Naftel DC, Pagani FD, et al. Seventh INTERMACS annual report: 15,000 patients and counting. *J Heart Lung Transpl* 2015;34:1495–504.
3. Crosby JR, DeCook KJ, Tran PL, et al. Physiological characterization of the SynCardia total artificial heart in a mock circulation system. *ASAIO J* 2015;61:274–81.
4. Grimm JC, Sciortino CM, Magruder JT, et al. Outcomes in patients bridged with univentricular and biventricular devices in the modern era of heart transplantation. *Ann Thorac Surg* 2016;102:102–8.
5. Levin AP, Jaramillo N, Garan AR, et al. Outcomes of contemporary mechanical circulatory support device configurations in patients with severe biventricular failure. *J Thorac Cardiovasc Surg* 2016;151:530–5.
6. Copeland JG, Smith RG, Arabia FA, et al. Cardiac replacement with a total artificial heart as a bridge to transplantation. *N Engl J Med* 2004;351:859–67.
7. Cohn WE, Timms DL, Frazier OH. Total artificial hearts: past, present, and future. *Nat Rev Cardiol* 2015;12:609–17.
8. Fox CS, McKenna KL, Allaire PE, Mentzer RM, Throckmorton AL. Total artificial hearts—past, current, and future. *J Card Surg* 2015;30:856–64.
9. Carpentier A, Latrémouille C, Cholley B, et al. First clinical use of a bioprosthetic total artificial heart: report of two cases. *Lancet* 2015;386:1556–63.
10. Pelletier B, Spiliopoulos S, Finocchiaro T, et al. System overview of the fully implantable destination therapy—ReinHeart-total artificial heart. *Eur J Cardiothorac Surg* 2014;47:80–6.
11. Healy AH, McKellar SH, Drakos SG, Koliopoulou A, Stehlik J, Selzman CH. Physiologic effects of continuous-flow left ventricular assist devices. *J Surg Res* 2016;202:363–71.
12. Shepherd RF, Ilievski F, Choi W, et al. Multigait soft robot. *Proc Natl Acad Sci U S A* 2011;108:20400–3.
13. Mac Murray BC, An X, Robinson SS, et al. Soft robotics: poroelastic foams for simple fabrication of complex soft robots. *Adv Mater* 2015;27:6334–40.
14. Ilievski F, Mazzeo AD, Shepherd RF, Chen X, Whitesides GM. Soft robotics for chemists. *Angew Chem Int Ed* 2011;123:1930–5.
15. Schumacher CM, Loepfe M, Fuhrer R, Grass RN, Stark WJ. 3D printed lost-wax casted soft silicone monoblocks enable heart-inspired pumping by internal combustion. *RSC Adv* 2014;4:16039–42.
16. Loepfe M, Schumacher CM, Stark WJ. Design, performance and reinforcement of bearing-free soft silicone combustion-driven pumps. *Ind Eng Chem Res* 2014;53:12519–26.
17. Roche ET, Wohlfarth R, Overvelde JTB, et al. A bioinspired soft actuated material. *Adv Mater* 2014;26:1200–6.
18. Ochsner G, Amacher R, Amstutz A, et al. A novel interface for hybrid mock circulations to evaluate ventricular assist devices. *IEEE Trans Biomed Eng* 2013;60:507–16.
19. Colacino FM, Moscato F, Piedimonte F, Arabia M, Danieli GA. Left ventricle load impedance control by apical VAD can help heart recovery and patient perfusion: a numerical study. *ASAIO J* 2007;53:263–77.
20. Heilmann C, Geisen U, Beyersdorf F, et al. Acquired von Willebrand syndrome in patients with ventricular assist device or total artificial heart. *Thromb Haemost* 2010;103:962–7.
21. Stamm C, Hetzer R, Total artificial heart. In: Bartunek J, Vanderheyden M, eds. *Translational Approach to Heart Failure*. New York, NY: Springer, 2013;437–48.
22. Basmadjian D, Sefton MV, Baldwin SA. Coagulation on biomaterials in flowing blood: some theoretical considerations. *Biomaterials* 1997;18:1511–22.
23. Farrar DJ, Hill JD, Pennington DG, et al. Preoperative and postoperative comparison of patients with univentricular and biventricular support with the thoratec ventricular assist device as a bridge to cardiac transplantation. *J Thorac Cardiovasc Surg* 1997;113:202–9.
24. Roussel JC, Sénage T, Baron O, et al. CardioWest (Jarvik) total artificial heart: a single-center experience with 42 patients. *Ann Thorac Surg* 2009;87:124–30.
25. Ghista DN, Vayo WH, Sandler H. Elastic modulus of the human intact left ventricle—determination and physiological interpretation. *Med Biol Eng Comput* 1975;13:151–61.
26. Slepian MJ, Alemu Y, Soares JS, Smith RG, Einav S, Bluestein D. The Syncardia™ total artificial heart: in vivo, in vitro, and computational modeling studies. *J Biomech* 2013;46:266–75.
27. Lubrizol Advanced Materials I. Isoplast(R) 2510 ETPU Technical Data Sheet, 2013.
28. Lubrizol Advanced Materials I. Isoplast(R) 2560 ETPU Technical Data Sheet, 2013.
29. Badeer HS. Hemodynamics for medical students. *Adv Physiol Educ* 2001;25:44–52.
30. Klotz S, Hay I, Dickstein ML, et al. Single-beat estimation of end-diastolic pressure-volume relationship: a novel method with potential for noninvasive application. *Am J Physiol Heart Circ Physiol* 2006;291:H403–H12.
31. Hall JE. *Guyton and Hall Textbook of Medical Physiology*, 13th Edition. Philadelphia, PA: Elsevier Health Sciences, 2015.
32. Timms D, Hayne M, McNeil K, Galbraith A. A complete mock circulation loop for the evaluation of left, right, and biventricular assist devices. *Artif Organs* 2005;29:564–72.
33. Nestler F, Bradley AP, Wilson SJ, Timms DL, Frazier OH, Cohn WE. A hybrid mock circulation loop for a total artificial heart. *Artif Organs* 2014;38:775–82.
34. Spzycher M. *High Performance Biomaterials: A Complete Guide to Medical and Pharmaceutical Applications*, 1st Edition. Lancaster, PA: Technomic Publishing AG, 1991.
35. McMillin CR. Characterization of Hexsyn, a polyolefin rubber. *J Biomater Appl* 1987;2:3–99.

SUPPORTING INFORMATION

Additional Supporting Information may be found in the online version of this article at the publisher's web-site:

Video S1. Recording of the soft total artificial heart (sTAH) on the hybrid mock circulation (18).

Fig. S1. Sketch of the soft total artificial heart with its outer dimensions in millimeters. c) depicts the

flow direction to and from the right ventricle (RV) and left ventricle (LV).

Fig. S2. Sketch of the main body of the soft total artificial heart with dimensions in millimeters.

Fig. S3. Sketch of the chambers of the soft total artificial heart with its outer dimensions in millimeters. LV, RV, and EC are abbreviations for left ventricle, right ventricle, and expansion chamber.

Fig. S4. Typical stress-strain curve of the used silicone elastomer.

Fig. S5. Scheme of the pneumatic actuation of the sTAH.

Fig. S6. Electric analog of the numerical model of the human blood circulation used for the evaluation of the soft total artificial heart (sTAH) on the modified hybrid mock circulation. The sTAH block is highlighted in grey in the figure to indicate where the interface is implemented.

Fig. S7. H-Q curves with three different prototypes of the soft total artificial heart.

Fig. S8. Preload variation experiment with two different prototypes of the sTAH. The signals of the pulmonary mean pressure (PVP), the aortic pressure (AoP) and the left heart flow (Q), as well as their mean values, are depicted.

Table S1. Summary of the minimum wall thicknesses of the soft total artificial heart

Table S2. Summary of the mechanical properties of the silicone elastomer mixture, which the sTAH is made of

Table S3. Summary of the inflation and deflation times for different physiological heart rates. The times also correspond to the opening and closing times of the expansion chamber-controlling valves

Table S4. Full list of experiments conducted with three soft total artificial hearts until rupture